
This is an electronic reprint of the original article.
This reprint may differ from the original in pagination and typographic detail.

Rasilainen, Kimmo; Lehtovuori, Anu; Viikari, Ville

On the operating principle of an LTE handset antenna with multiple closely-located radiators

Published in:

12th European Conference on Antennas and Propagation (EuCAP 2018)

DOI:

[10.1049/cp.2018.1162](https://doi.org/10.1049/cp.2018.1162)

Published: 01/01/2018

Document Version

Peer-reviewed accepted author manuscript, also known as Final accepted manuscript or Post-print

Please cite the original version:

Rasilainen, K., Lehtovuori, A., & Viikari, V. (2018). On the operating principle of an LTE handset antenna with multiple closely-located radiators. In *12th European Conference on Antennas and Propagation (EuCAP 2018)* European Association on Antennas and Propagation (EurAAP). <https://doi.org/10.1049/cp.2018.1162>

This material is protected by copyright and other intellectual property rights, and duplication or sale of all or part of any of the repository collections is not permitted, except that material may be duplicated by you for your research use or educational purposes in electronic or print form. You must obtain permission for any other use. Electronic or print copies may not be offered, whether for sale or otherwise to anyone who is not an authorised user.

On the Operating Principle of an LTE Handset Antenna with Multiple Closely-Located Radiators

Kimmo Rasilainen, Anu Lehtovuori, and Ville Viikari

Department of Electronics and Nanoengineering, Aalto University School of Electrical Engineering,
P.O. Box 15500, FI-00076 AALTO, Finland
firstname.lastname@aalto.fi

Abstract—Analysis of the operating and design principles of an LTE handset antenna is carried out. The antenna utilises a combination of fed and aperture-matched radiators that are located close to each other physically and electrically. These radiators, together with fixed matching circuits, provide good matching and efficiency performance at LTE frequencies 698–960 MHz and 1.7 GHz upwards. The effect of individual parts or components on the antenna performance is analysed. Results of the current work provide general design rules that can be applied to other implementations as well, with an emphasis on getting as good a low-band performance as possible.

Index Terms—antenna, aperture matching, efficiency, handset, mutual coupling.

I. INTRODUCTION

In both current and future-generation handsets, requirements for, e.g., more supported radio systems and higher data rates place challenges also for the antenna design. Meeting these requirements calls for more advanced hardware solutions, and also for the use of Multiple-Input, Multiple-Output (MIMO) communications. In the MIMO scheme, the number of antennas increases inside the handset, which reduces the inter-antenna distance and increases the mutual coupling.

One solution to the MIMO-related challenges is to use tunable antennas covering only part of the required frequency bands at a time [1]. Such antennas can be more robust to the effects of mutual coupling, but the required tunable circuit components (typically capacitors) are problematic from the point of view of Carrier Aggregation (CA). In CA, antennas communicate with multiple, narrow component carriers (CC). The different CCs can be at the same frequency band (intra-band CA) or at different bands (inter-band CA). Non-linear effects associated with changing the state of the tunable component can cause new, unwanted frequencies that may occur at the various CCs.

A somewhat opposite strategy is to make use of the mutual coupling of closely-located antennas rather than to avoid it. The mutual coupling can occur between adjacent antennas or between different feeds connected to the same antenna [2], [3]. Recent works have shown designs that use combinations of closely-located fed, aperture-matched, and fully parasitic radiators in various configurations [4], [5]. This kind of design is also referred to as a Combined Parasitic-coupled, Aperture-Matched (CPAM) antenna [5]. With this concept, it is possible

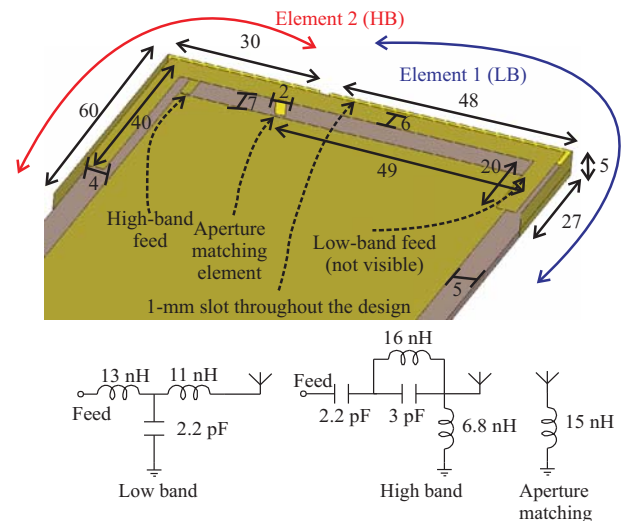


Fig. 1. Illustration of the three-element antenna and matching circuits of [4]. The third, C-shaped element is located above the substrate. All dimensions are in millimetres. Circuit element values represent those of realistic Murata capacitors and inductors.

to achieve instantaneous coverage of the LTE low band (698–960 MHz) with passive matching circuits, which makes this approach CA compatible.

However, the fundamental, underlying mechanisms behind the operation of the CPAM antenna are not analysed in detail in [4], [5]. The current investigation extends the work of [4] by considering the individual contribution of the parasitic elements and aperture matching on the overall antenna performance at the low and high bands (LB and HB, respectively). This study is performed using electromagnetic and circuit simulations, and the improved understanding gained from the analysis can be utilised to identify the essential properties needed to design well-performing antennas with inherently strong mutual coupling.

II. INVESTIGATED ANTENNA AND MATCHING CIRCUIT DESIGNS

The antenna structure analysed in this work, and originally presented in [4], has three radiators that are located close to each other both physically and electrically. Fig. 1 illustrates this design together with the matching circuits used (taken

from [4]). All antennas are implemented for a handset with dimensions $80 \times 160 \times 5 \text{ mm}^3$ (width \times length \times height), and these are comparable to current high-end smartphones.

None of the three radiators are physically connected together, and there is a constant slot between each part. Through the feeds and grounding components, the radiators are connected to the same chassis. Realistic capacitor and inductor models based on S -parameters are utilised for the matching circuits in the simulations, and Murata components are applied. The antennas are designed for an FR-4 substrate ($\epsilon_r = 4.4$), whose thickness is 1.5 mm, and the effect of material parameters (including metal and dielectric losses) is taken into account.

In the design of [4], the antenna has separate low- and high-band feeds, which are matched using low- and high-pass type matching circuits, respectively. These feeds are exciting the L-shaped antenna elements around the corners of the device. The third, C-shaped radiator is positioned above the substrate, at the same plane as the upper edge of the L-elements. The C-element is used for aperture matching, and it is not fed. This kind of feed configuration provides good isolation between the low- and high-band elements.

III. ANALYSIS OF THE ANTENNA PERFORMANCE

The effect of different antenna parts on the overall performance is analysed in the following. Investigations are made in terms of impedance matching, mutual coupling, and efficiency. The antenna response is constructed in three main steps to see the contribution of: 1) the corner-located L-shaped elements, 2) a fully parasitic C-shaped element, and 3) the aperture matching applied to the C-element.

A. Corner-Located L-Shaped Elements (Step 1)

Of the antenna parts shown in Fig. 1, we first consider the L-shaped corner radiators. In the final design, elements 1 and 2 are used to implement the low- and high-band operation, respectively. Fig. 2 illustrates the input matching and mutual coupling of these antennas with and without the matching circuits. The response of element 1 has a strong resonance around 1.7 GHz. At this frequency, the length of the element is approximately $\lambda/2$. The 'dipole mode' can also be seen in the current distribution. On the other hand, element 2 represents a frequency response more typical for a Capacitive Coupling Element (CCE) structure, which can be matched across a wide range of frequencies with a suitable matching circuit [6].

The Smith chart plot of Fig. 2 shows that the impedance of element 1 remains capacitive across the entire low band, whereas that of element 2 becomes inductive after 850 MHz. This means that it is more straightforward to use element 1 as the low-band radiator by applying a suitable, inductive matching circuit. Comparison of the curves in Fig. 2 shows that at the low band, the performance of elements 1 and 2 is quite similar without the matching circuits. Matching the antenna elements significantly decreases the mutual coupling at the targeted bands, especially at the low band.

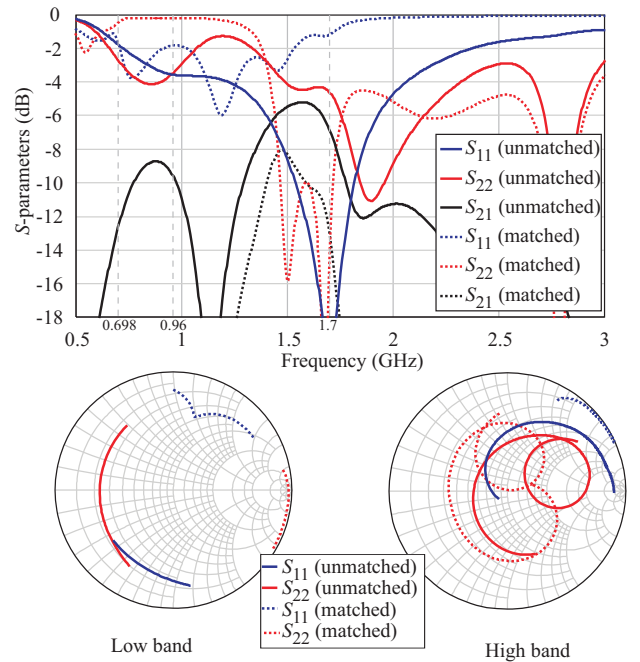


Fig. 2. Antenna S -parameters with the low- and high-band L-shaped elements. Port 1 = LB, Port 2 = HB.

B. Parasitic C-Shaped Element (Step 2)

As the following step, the aim is to improve the performance of the antenna at the low band through better matching. With the currently used matching circuits and corner-located antenna elements, element 1 is too small to operate efficiently at frequencies below 1 GHz, which can also be seen in the results of Fig. 2. One solution to improve the operation could be to use elements 1 and 2 simultaneously with a different matching scheme to provide good matching at the low band, while still trying to maintain the good high-band performance and isolation. Here, we analyse an alternative approach that increases the volume of the antenna by placing a C-shaped radiator above the substrate and near the corner elements.

By having the C-element in the vicinity of the corner radiators, the operation of the antenna improves due to the additional coupling introduced by the C-element. There is a constant, 1-mm slot between the L- and C-shaped elements (see Fig. 1), and therefore the additional benefit is caused by coupling through the fields between the individual parts. Additionally, the slot helps to keep the overall coupling at a moderate level. Fig. 3 presents the performance of the antenna in the presence of the C-element with and without the matching circuits. As shown in Fig. 3, and discussed previously in [4], having one band matched and the other one mismatched in the individual feeds provides very good performance.

The combined effect of the C-element and the slot increases the effective size of element 1, which is beneficial for the low-band performance, and a matching level of better than -4 dB is achieved at the low band with proper matching circuits. It should be noted that without the matching networks, elements

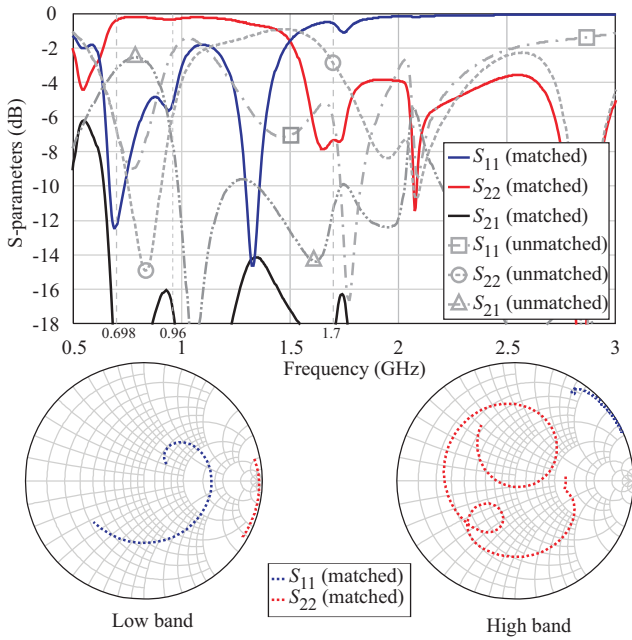


Fig. 3. Effect of adding a fully parasitic C-shaped element above the corner radiators. Port 1 = LB, Port 2 = HB.

1 and 2 both exhibit a pronounced low-band resonance, which results in very high mutual coupling levels. This can be seen in the grey curves of Fig. 3.

C. Effect of Aperture Matching (Step 3)

As the curves of Fig. 3 show, the antenna impedance already rotates quite nicely around the Smith chart at the low band in the presence of the parasitic C-element. By enhancing the low-band matching, the impedance loop could be brought closer to the centre of the Smith chart. To achieve this, the parasitic C-element is grounded to the chassis through an inductor.

Aperture matching is used to tune the resistance and reactance of the antenna by adding additional feeding/shorting pins or lumped components to the antenna [7]–[10]. Typically, this approach is applied across a single antenna element; the current three-element design can effectively be considered as a single radiator due to the inherent coupling levels. The goal of modifying the antenna impedance is to facilitate the matching at desired frequencies. In the currently analysed design, the aperture matching is done through the grounding inductor.

As illustrated in Fig. 4, applying the aperture matching provides very good instantaneous coverage at the low band, and the matching level is better than -6 dB. The high-band performance does not significantly change by introducing the aperture-matching inductor. A comparison of Figs. 2–4 shows that the changes in Steps 1–3 mainly contribute to getting a good low-band operation. In the aperture-matched case, element 2 achieves a high-band impedance matching level of -4 dB across the entire LTE high band (1710–2690 MHz), which falls a bit short of the -6 dB matching criterion typically considered when designing handset antennas. On the other

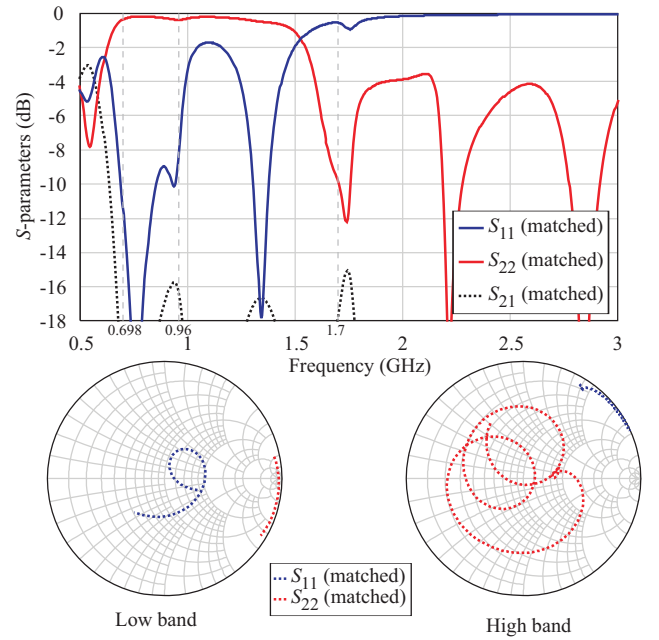


Fig. 4. Effect of grounding the C-element with an inductor (aperture matching). Port 1 = LB, Port 2 = HB.

hand, practical antenna designs, e.g., for commercial products, tend to emphasise the efficiency rather than matching [11].

D. Antenna Efficiency

In the previous part, the matching and mutual coupling performance of the design presented in [4] has been analysed. Efficient antenna performance requires both of these parameters to be at a suitable level, which can be seen in the expression of embedded radiation efficiency calculated from the S -parameters [12]

$$e_{\text{rad},i} = 1 - |S_{ii}|^2 - \sum_{i \neq j} |S_{ij}|^2. \quad (1)$$

This expression takes into account both the matching of individual antenna ports (the ii terms) and coupling between different ports (the ij terms). As an example, a two-element design with good matching at both ports will not have good efficiency if the power couples between the ports due to poor isolation rather than radiates from the antenna structure.

Therefore, the next thing is to consider the effect of the proposed design steps on the antenna efficiency. For the different intermediate steps, the e_{rad} values are calculated. Additionally, the radiation (η_{rad}) and total (η_{tot}) efficiencies are determined from the simulated far fields for the final antenna design.

Fig. 5(a) presents the calculated e_{rad} results for the matched corner elements and when the parasitic C-element is included in the design. The curves show that at the low band, including the C-element is required to achieve feasible e_{rad} values better than 60% across the band. When comparing the efficiency results to the S -parameters, it is clear that the most significant improvement between the design steps is caused by enhanced

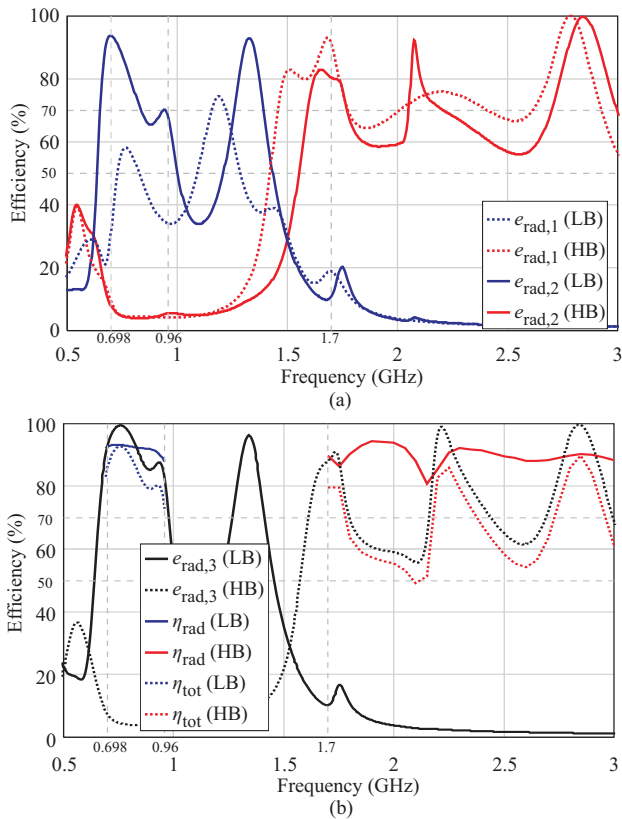


Fig. 5. (a) Embedded radiation efficiency (e_{rad}) calculated from S -parameters after steps 1 and 2. (b) Calculated e_{rad} for the entire structure (after step 3), and radiation (η_{rad}) and total (η_{tot}) efficiency of the antenna determined from the far fields.

matching, as the coupling between the low- and high-band ports remains low throughout the design.

At the high band, similar observations can in general be made. Here, due to a better initial matching level, the design provides higher than 60% embedded radiation efficiency even without the C-element. In fact, the parasitic element makes the high-band efficiency slightly worse, but the resulting improvement at the low band more than compensates for this.

For the entire structure, Fig. 5(b) illustrates for comparison both the e_{rad} performance and the η_{rad} and η_{tot} results for the low and high bands. In terms of e_{rad} , introducing the aperture matching clearly improves the efficiency at the LTE low band, where it is now better than 80%. At the low and high bands, the far field η_{tot} result follows the shape of the e_{rad} curve, but the values are slightly lower. This is an expected result, as the e_{rad} is purely valid for total (radiation) efficiency in the case of lossless antennas [12]. The performance of the antenna analysed in this work is very good in terms of matching and efficiency, especially at the low band.

IV. CONCLUSION

This paper has analysed the operation of an LTE handset antenna with closely-located radiators and fixed matching circuits. Effects of impedance matching, parasitic radiators and

the use of aperture matching have been considered, as well as the individual contribution of these factors to the performance of the final design. The antenna structure is analysed at both low and high bands, and achieving good operation with the current configuration of radiators, especially at the low band, requires using a combination of fed elements and aperture-matched parasitic radiators. Additional understanding gained on the basic operating principles of an antenna with closely-located radiators can be utilised to design well-performing antennas also for other designs and applications where inherently strong mutual coupling is observed.

ACKNOWLEDGEMENT

This work was conducted within the 5G TRx research project funded by TEKES (The Finnish Funding Agency for Technology and Innovation), Nokia Solutions and Networks, RF360, Microsoft Mobile, Sasken Finland, Pulse Finland, and Huawei Technologies Finland, and by the Academy of Finland under Decision 289320. The work of K. Rasilainen was supported in part by the Aalto ELEC Doctoral School, by the Nokia Foundation, and by the KAUTE Foundation.

REFERENCES

- [1] S. Caporal del Barrio, A. Morris, and G. F. Pedersen, "Addressing carrier aggregation with narrow-band tunable antennas," *2016 10th European Conference on Antennas and Propagation (EuCAP)*, Davos, Switzerland, Apr. 2016, 5 p.
- [2] Z. Bao, Z. Nie, and X. Zong, "A novel broadband dual-polarization antenna utilizing strong mutual coupling," *IEEE Trans. Antennas Propag.*, vol. 62, no. 1, pp. 450–454, Jan. 2014.
- [3] R. Valkonen, M. Kallio, and C. Icheln, "Capacitive coupling element antennas for multi-standard mobile handsets," *IEEE Trans. Antennas Propag.*, vol. 61, no. 5, pp. 2783–2791, May 2013.
- [4] K. Rasilainen, A. Lehtovuori, and V. Viikari, "LTE handset antenna with closely-located radiators, low-band MIMO, and high efficiency," *2017 11th European Conference on Antennas and Propagation (EuCAP)*, Paris, France, Mar. 2017, pp. 3074–3078.
- [5] K. Rasilainen, A. Lehtovuori, A. Boussada, and V. Viikari, "Carrier aggregation compatible MIMO antenna for LTE handset," *Progress In Electromagnetics Research C*, vol. 78, pp. 1–10, 2017.
- [6] J. Villanen, J. Ollikainen, O. Kivekäs, and P. Vainikainen, "Coupling element based mobile terminal antenna structures," *IEEE Trans. Antennas Propag.*, vol. 54, no. 7, pp. 2142–2153, Jul. 2006.
- [7] S. Park, H. Kim, H. Choi, J. Cho, and H. Kim, "A design of multi band chip antenna with the shorting pin for mobile handsets," *2007 2nd European Conference on Antennas and Propagation (EuCAP)*, Edinburgh, UK, Nov. 2007, 4 p.
- [8] W. Lee, M. Ko, J. Kim, and Y. J. Yoon, "Analysis of the shorting pin effects on an inverted-F antenna using an equivalent model for impedance matching," *2010 4th European Conference on Antennas and Propagation (EuCAP)*, Barcelona, Spain, Apr. 2010, 5 p.
- [9] S. M. Ali and K. Payandehjoo, "Tunable antenna techniques for compact handset applications," *IET Microw. Antennas Propag.*, vol. 8, no. 6, pp. 401–408, Apr. 2014.
- [10] T.-W. Kang and K.-L. Wong, "Chip-inductor-embedded small-size printed strip monopole for WWAN operation in the mobile phone," *Microw. Opt. Technol. Lett.*, vol. 51, no. 4, pp. 966–971, Apr. 2009.
- [11] A. Lehtovuori, J. Ilvonen, K. Rasilainen, and V. Viikari, "Single-element handset antenna design for modern smartphones: An industrial approach," *2017 11th European Conference on Antennas and Propagation (EuCAP)*, Paris, France, Mar. 2017, pp. 2960–2963.
- [12] P.-S. Kildal, *Foundations of Antenna Engineering: A Unified Approach for Line-Of-Sight And Multipath*, Kildal, 2015.